Near-Field Scanning Microwave Microscopy of Superconducting Materials and Devices

Steven M. Anlage[1], A. S. Thanawalla[1], A. P. Zhuravel'[2], W. Hu[1], C. P. Vlahacos[1], D. E. Steinhauer[1], S. K. Dutta[1], and F. C. Wellstood [1]

[1]Center for Superconductivity Research and Materials Research Science and Engineering Center, Physics Department, University of Maryland, College Park, MD 20742-4111 USA.
[2]B. I. Verkin Institute for Low Temperature Physics and Engineering, Academy of Sciences of the Ukraine, 47 Lenin Avenue, 310164 Kharkov, Ukraine.

Abstract: Superconducting microwave devices are now beginning to show significant potential for cellular telephone applications. The key limitations to this new technology, besides reliable inexpensive cryogenic cooling, are the problems of power dependence and nonlinearity. We have employed imaging techniques, including scanning near-field microwave microscopy of devices and materials, to begin examining the microscopic origins of nonlinearity.

Key words: Microwave Microscopy, Near-Field, Superconducting Materials, Superconducting Microwave Devices, Intermodulation

Introduction. The use of superconducting microwave devices for the cellular telephone market could become the first example of the large scale application of high-temperature superconducting devices. However, the use of superconductors under the high power conditions encountered in radar transmitters (or receivers in a jamming environment), and cellular base station transmitters, is not feasible at present. The main problem is control of the power dependence and nonlinearities inherent in present-day high-T_C devices. In the past, efforts to control these problems have been entirely empirical, although moderately successful. However, the commercial superconducting microwave community has largely postponed its efforts to understand the power dependence and nonlinearity, because of the pressing need to scale-up production and complete existing device development and testing. Here, we describe our work towards understanding the microscopic origins of microwave power dependence and nonlinearity, with the purpose of significantly improving the power-handling capabilities of superconducting microwave devices.

The Problem of Power Dependence and Nonlinearity. During the early stages of microwave measurements on high-T_C bulk materials and thin films, it was seen that the surface impedance was highly dependent upon the level of RF field excitation. This early work also identified the main source of power dependence as being due to decoupling of grains by intergranular RF magnetic flux, and the subsequent hysteretic response of rf flux flow through the resulting junction [1]. Efforts were made to identify the microscopic origin of these hysteretic junctions [2]. Weakly coupled grains in bulk materials and polycrystalline films were identified as culprits. However, as epitaxial c-axis oriented thin films of $YBa_2Cu_3O_{7-\delta}$ (YBCO) became widely available, it was found that high residual losses and strong power dependence persisted.

Power dependence of the microwave properties translates into significant problems when superconducting microwave devices are used in real applications. One major problem (even at low power) is intermodulation of two or more signals, caused by nonlinearities in these devices. A measure of this nonlinearity is provided by the Third-Order Intercept (TOI) of a device. If two signals at different frequencies (say f_1 and f_2) are simultaneously applied to a device, a third-order signal, such as that at $2f_1 - f_2$, will be generated due to nonlinearities. The power in the third order mode is monitored as a function of the power input at f_1 and f_2, and usually has slope 3 on a log-log plot. The extrapolated input power at which the third order output power equals the extrapolated input power is called the third order intercept. The higher the TOI, the better the device.

Many groups routinely measure the TOI of their devices. However, this is a "black box" measurement: one has no idea how the nonlinearities are created, or where they are being generated in the device. As a result, there are several outstanding mysteries about the high-T_c TOI data:

1) The TOI's are much lower than those obtained with normal-metal devices, making high-T_c devices significantly less attractive than existing devices.

2) The slope of the third order output is often not equal to 3, as expected from theory,[3] but is often 2.5 or smaller. A possible origin of this weaker power dependence is a nonlinear inductance which changes from an I_{rf}^2 dependence to a $|I_{rf}|$ dependence [4]. The reason for this change may be due to flux entry at weak links, but is still unknown.

3) The third order output sometimes "jogs" over, producing superior performance for a time before, for some unknown reason, [3],[5] resuming a slope-3 behavior.

The Need for Microscopic Imaging of Fields and Currents. The state-of-the-art in superconducting microwave device research is summarized in two quotes from an August 1997 report entitled "New Research Opportunities in Superconductivity." "There is virtually no understanding of the relationship between material defects and RF conductivity."[6] Also, "[t]here has been as yet no success in measuring the RF conductivity and/or its nonlinearity with high spatial resolution (i.e. on sub-micron scales). This is sorely needed to begin to understand the role of defects."[6]

New tools are required to make progress in bringing power dependence and nonlinearity under control. The key is to image the flow of rf current on the length scale comparable to the magnetic penetration depth. The imaging must be done for rf current flow, as dc currents will flow differently and will lack important characteristics associated with inductive or capacitive effects. Coupled with this, we also need a local probe of microstructure of these devices, to see which defects are most disruptive and which are relatively benign.

It is well known that rf and dc currents flowing in superconducting transmission lines show a significant degree of "current crowding" near the edges of the film (see Fig. 1). It is believed that at high rf current density the superconducting films break down at the edges, and allow rf magnetic flux to move in and out of the film at the edge [2]. This hysteretic process leads to significant additional loss, and to an increase in the inductance of the circuit. Both of these consequences are detrimental to the operation of the device. The situation will become even worse as devices with higher characteristic impedance (50 Ω and 75 Ω) are built, as they require narrow signal lines. The narrower lines will increase the current crowding, as well as magnify the effects of granularity and defects in the film.

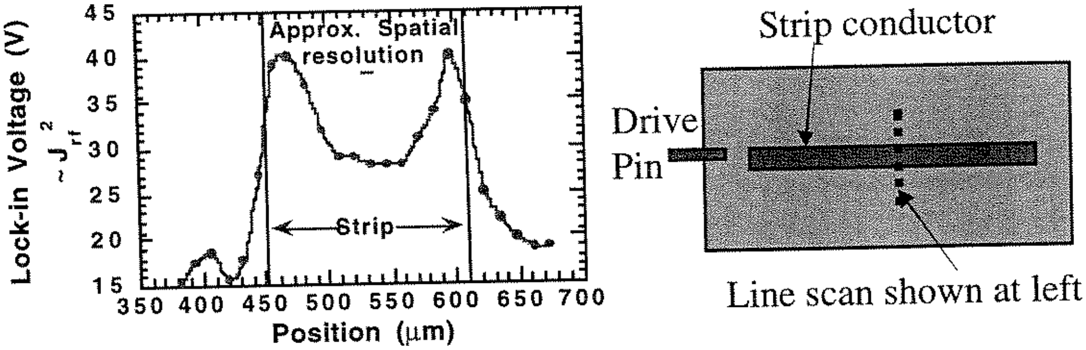

Fig. 1. Scanning laser microscope line scan taken across a $Tl_2Ba_2CaCu_2O_8$ superconducting microstrip transmission line resonator at its fundamental mode of 8.2 GHz and at a temperature T ~ 100 K, several degrees below T_c. The signal is proportional to the local rf current density squared, and shows current crowding at the edges.

Our preliminary efforts to image the current distribution on a microstrip transmission line are shown in Fig. 1. The image is made with a laser-based far-field microwave microscope similar to that used by Culbertson and Newman to image the supercurrent distribution due to bolometric changes in the magnetic penetration depth [7]. On resonance, the current at a given point in the resonator is given by $J(t) = J_0 \cos(\omega t)$. In the presence of a low-frequency modulated laser beam, there will be a change in the local magnetic penetration depth of the film due to the local heating, given by, $\lambda(t) = \lambda_0 + \Delta\lambda \cos^2(\omega' t)$, where ω' is the modulation frequency of the laser light The change in resonant frequency due to the thermal perturbation is given by; $\Delta f/f_0 = -\Delta U/U \sim \lambda^2 J^2 \Delta\lambda A$, where J is the local current density and A is the area heated by the laser beam [7]. Hence a small change in the local penetration depth of the film will cause a change in resonant frequency, f_0, of the device which is proportional to the local current density squared. By scanning the position of the laser beam about the sample, and measuring the change in resonant response, one can map out the current distribution in the superconducting resonator. The image in Fig. 1 was taken with a laser intensity modulation frequency of f'= 1 kHz and a spot diameter of 10 to 15 μm.

Scanning Near-Field Microwave Microscopy. Our main approach to the problem of nonlinearity in superconducting devices is to use near-field microwave microscopy techniques. Near field microwave measurements have been pursued by many groups over the years. The earliest work by Soohoo [8] and Bryant and Gunn [9] used scanned resonators with small apertures to couple to the sample of interest. The method of Ash and Nichols used an open resonator formed between a hemispherical and planar mirror [10]. They opened a small hole in the planar mirror allowing an evanescent wave to leave the cavity and scanned a sample beneath it. Near-field imaging has also been accomplished using evanescent waves from the optical to the microwave range in coaxial, waveguide, microstrip, and scanning tunneling microscope geometries [11]-[17].

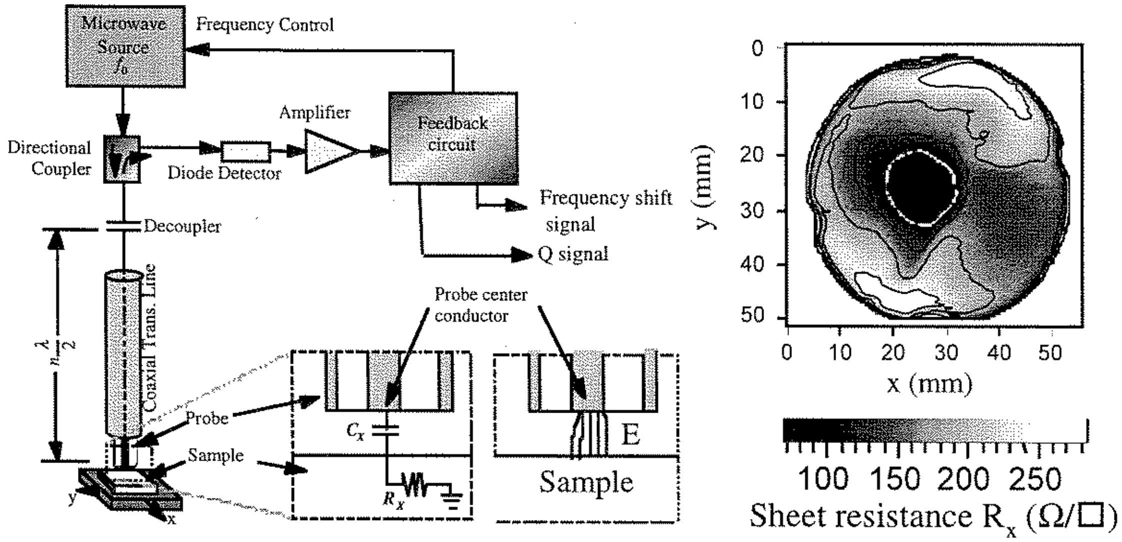

Fig. 2. (Left) Schematic of materials diagnostics scanning near-field microwave microscope. The insets show a simple model of the probe / sample interaction, as well as the concentrated electric fields below the center conductor of the open-ended coaxial probe. (Right) Quantitative surface sheet resistance (in Ω/□) image of a 2" diameter sapphire wafer covered with an $YBa_2Cu_3O_7$ thin film. The image is taken at room temperature with a 480 μm probe at a height of 50 μm and at a frequency of 7.5 GHz. From Ref. [18].

Over the past few years, our group has developed several novel forms of near-field scanning microwave microscopy. Our system works by scanning a fine open-ended coaxial probe over a sample. These microscopes have two basic operating modes: materials diagnostic imaging and electromagnetic field imaging.

Material Diagnostic Imaging. As shown in Fig. 2, in a material diagnostic mode, a resonant coaxial cable is weakly coupled to a microwave generator on one end through a decoupling capacitor C_d, and coupled to a sample through an open-ended coaxial probe on the other end. As the sample is scanned beneath the probe, the capacitive coupling to the sample, C_x, will vary due to dielectric changes or topography. This has the result of changing the resonant frequency of the resonant cable. Also, as the local sheet resistance (R_x) of the sample varies, so will the quality factor, Q, of the resonant cable. A feedback circuit can be used to force the microwave generator to follow a single resonant frequency of the cable, and a second circuit can be used to monitor the Q of the circuit, both in real time. Hence as the sample is scanned below the open-ended coaxial probe, the frequency shift and Q signals are collected, and a two-dimensional image of the sample topography and sheet resistance are recorded. Our feedback circuit runs fast enough to accurately record at scan speeds of up to 25 mm/sec.

As with other forms of near-field microscopy, the probe is placed well within one wavelength of the sample under study. This is particularly easy to accomplish at rf, microwave, and millimeter-wave frequencies because the wavelengths range from meters to millimeters. However, the spatial resolution of our microscopes also depends on the probe-sample separation; the spatial resolution of such a microscope is the larger of the probe-sample separation and the diameter of the inner conductor wire in the open-ended coaxial cable [19],[20]. To achieve fine resolution, we must place the probe closer to the sample, and maintain a constant separation. Using our current instruments, we have achieved a spatial resolution of approximately 10 μm without dragging the probe across the sample, and better than 1 μm in contact mode [19]-[22].

Our scanning near-field microwave microscope can be used to obtain quantitative topographic images with 50 nm vertical sensitivity,[23] quantitative surface sheet resistance images,[18] and quantitative ε_r images [24]. For example, Fig. 2 shows a sheet resistance image of a $YBa_2Cu_3O_7$ thin film deposited on a 2" diameter sapphire wafer. The film shows a sheet resistance which varies by a factor of 3 over its surface. The image was obtained at room temperature in only 10 minutes.

Electromagnetic Field Imaging. One can also use the open-ended coaxial probe to pick-up electric fields above an operating device. We have imaged a variety of devices, including quantitative electric field (at the probe tip) images above a Cu and superconducting $Tl_2Ba_2CaCu_2O_8$ microstrip resonators at 77 K with a cryogenic microscope.[25],[26] By performing measurements at various heights above the sample, we can reconstruct the field profile, and then calculate the electric potential everywhere above the devices. However, we find that the measured electric field values are strongly enhanced over their unperturbed values.

There are two important questions which are currently unanswered about electromagnetic field images. First is how to properly calibrate the images in terms of the unperturbed electric or magnetic field. The second unanswered question is the degree of perturbation caused by the probes as they sample the electric and magnetic fields of a device. We have recently developed a feedback loop which continuously adjusts the source to excite the perturbed device on resonance [26]. We have found that the coaxial probe perturbs the electric fields which we are trying to image. One conclusion is that the fields are typically enhanced by a factor on the order of 10^2 over the values of the field in the absence of the probe,[25] depending on the distance between the probe and the sample.

Conclusions. The microscopic imaging approach to solving the problem of nonlinearity in superconducting microwave devices shows great promise. Scanning laser microscopes can probe the microwave current distribution on micron length scales. Scanning near-field microwave microscopes are sensitive to variations in sheet resistance, dielectric constant and topography on comparable length scales. Finally, our microwave microscopes can also be used to image microwave electromagnetic fields of operating superconducting microwave devices under cryogenic conditions, giving a new window into their operation.

Acknowledgements. This work is supported by NSF through grants ECS-9632811, and MRSEC DMR-9632521, NATO through grant HTECH.EV 971764, and the Maryland Center for Superconductivity Research.

REFERENCES

1. A. M. Portis, *et al.*, Appl. Phys. Lett. 58, 307 (1991).
2. T. C. L. Gerhard Sollner, J. P. Sage, and D. E. Oates, Appl. Phys. Lett. 68, 1003 (1996); D. E. Oates, *et al.*, Appl. Phys. Lett. 68, 705 (1996).
3. Zhi-Yuan Shen, High-Temperature Superconducting Microwave Circuits, (Artech House, Boston), 1994.
4. Balam Willemsen, Talk ESB-03, 1998 Applied Superconductivity Conference, Palm Desert, CA.
5. Private communication with Z. Y. Shen and C. Wilker of Dupont.
6. New Research Opportunities in Superconductivity IV, a report on the Workshop on Research Needs and Opportunities in Superconductivity, B. J. Batlogg, R. A. Buhrman, J. R. Clem, D. U. Gubser, D. C. Larbalestier, D. H. Liebenberg, J. M. Rowell, R. E. Schwall, D. T. Shaw, and A. W. Sleight, Monterey, CA, 10 - 12 February, 1997.
7. H. S. Newman, and J. C. Culbertson, Microwave Opt. Tech. Letts. 6, 725 (1993).
8. R. F. Soohoo, J. Appl. Phys. 33, 1276 (1962).
9. C. A. Bryant and J. B. Gunn, Rev. Sci. Instrum. 36, 1614 (1965).
10. E. A. Ash and G. Nicholls, Nature 237, 510 (1972).
11. M. Tabib-Azar, N. S. Shoemaker and S. Harris, Meas.Sci. Tech. 4, 583 (1993).
12. T. Wei, X. D. Xiang, W. G. Wallace-Freedman, and P. G. Schultz, Appl. Phys. Lett. 68, 3506 (1996).
13. R. J. Hamers, and D. G. Cahill, Appl. Phys. Lett. 57, 2031 (1990).
14. I. Takeuchi, *et al.*, Appl. Phys. Lett. 71, 2026 (1997).
15. S. J. Stranick, L. A. Blumm, M. M. Kamma, and P. S. Weiss, in *Photons and Local Probes*, edited by O. Marti and R. Miller (Kluwer, Netherlands, 1995), p. 221.
16. F. Keilmann, D. W. van der Weide, T. Eickelkamp, R. Merz, and D. Stakle, Opt. Commun. 129, 15 (1996).
17. M. Fee, S. Chu, and T. W. Hansch, Optics Commun. 69, 219 (1989).
18. D. E. Steinhauer, C. P. Vlahacos, Sudeep Dutta, F. C. Wellstood, and Steven M. Anlage, Appl. Phys. Lett. 71, 1736 (1997). cond-mat/9712142.
19. C. P. Vlahacos, R. C. Black, S. M. Anlage and F. C. Wellstood, Appl. Phys. Lett. 69, 3272 (1996).
20. Steven M. Anlage, C. P. Vlahacos, Sudeep Dutta, and F. C. Wellstood, IEEE Trans. Appl. Supercond. 7, 3686 (1997).
21. B. J. Feenstra, C. P. Vlahacos, Ashfaq S. Thanawalla, D. E. Steinhauer, S. K. Dutta, F. C. Wellstood and Steven M. Anlage, 1998 IEEE MTT-S Proceedings, page 965, June, 1998. cond-mat/9802293.
22. D. E. Steinhauer, C. P. Vlahacos, S. K. Dutta, B. J. Feenstra, F. C. Wellstood, and Steven M. Anlage, Appl. Phys. Lett. 72, 861 (1998). cond-mat/9712171.
23. C. P. Vlahacos, D. E. Steinhauer, S. K. Dutta, B. J. Feenstra, Steven M. Anlage, and F. C. Wellstood, Appl. Phys. Lett., 72, 1778 (1998). cond-mat/9802139.
24. C. P. Vlahacos, D. E. Steinhauer, S. K. Dutta, B. J. Feenstra, Steven M. Anlage, and F. C. Wellstood, submitted to Appl. Phys. Lett., October, 1998.
25. S. K. Dutta, C. P. Vlahacos, D. E. Steinhauer, Ashfaq S. Thanawalla, B. J. Feenstra, F. C. Wellstood and Steven M. Anlage, Appl. Phys. Lett., January 4, 1999.
26. Ashfaq S. Thanawalla, S. K. Dutta, C. P. Vlahacos, D. E. Steinhauer, B. J. Feenstra, Steven M. Anlage, and F. C. Wellstood, Appl. Phys. Lett., 73, 2491 (1998).

NO
CO

Kenta

Depar
464-8

ABS

We in
thin f
analy
mina
Y:Ba:
an M
thin f

KE

INT

It is
Espe
chan
cont
it is
accu
To s
ton
gen
NR
3.04
The
film
Å is

EX